
White Rose Research Online

eprints@whiterose.ac.uk
https://eprints.whiterose.ac.uk
Universities of Leeds, Sheffield and York

Deposited via The University of Leeds.

White Rose Research Online URL for this paper:
https://eprints.whiterose.ac.uk/id/eprint/111507/

Version: Accepted Version

Article:
Nelson, DJ, Gichuhi, WK, Miller, EM et al. (2017) Anion Photoelectron Spectroscopy of Deprotonated ortho-, meta-, and para-methylphenol. Journal of Chemical Physics, 146 (7). 074302. ISSN: 0021-9606

https://doi.org/10.1063/1.4975330

© The Authors 2017. The following article appeared in Journal of Chemical Physics 146(7) Article number 074302 on 15 Feb 2017 and may be found at https://doi.org/10.1063/1.4975330. This article may be downloaded for personal use only. Any other use requires prior permission of the author and AIP Publishing.

Reuse
Items deposited in White Rose Research Online are protected by copyright, with all rights reserved unless indicated otherwise. They may be downloaded and/or printed for private study, or other acts as permitted by national copyright laws. The publisher or other rights holders may allow further reproduction and re-use of the full text version. This is indicated by the licence information on the White Rose Research Online record for the item.

Takedown
If you consider content in White Rose Research Online to be in breach of UK law, please notify us by emailing eprints@whiterose.ac.uk including the URL of the record and the reason for the withdrawal request.



Anion Photoelectron Spectroscopy of Deprotonated *ortho*-, *meta*-, and *para*-Methylphenol

Daniel J. Nelson,[1] Wilson K. Gichuhi,[1,2] Elisa M. Miller,[1,3] Julia H. Lehman,[1,4] and W. Carl Lineberger[1*]

[1]*JILA and Department of Chemistry and Biochemistry, University of Colorado, Boulder, CO 80309, United States of America*

[2]*Present address: Department of Chemistry, Tennessee Tech University, Cookeville, TN 38505, United States of America*

[3]*Present address: Chemical and Materials Sciences Center, National Renewable Energy Laboratory, Golden, CO 80401, United States of America*

[4]*Present address: School of Chemistry, University of Leeds, Leeds LS2 9JT, United Kingdom*

*Corresponding Author email: Carl.Lineberger@Colorado.edu.

ABSTRACT

The anion photoelectron spectra of *ortho-, meta-,* and *para*-methylphenoxide, as well as methyl deprotonated *meta*-methylphenol, were measured. Using the Slow Electron Velocity Map Imaging (SEVI) technique, the Electron Affinities (EAs) of the *o-, m-,* and *p*-methylphenoxyl radicals were measured: 2.1991 ± 0.0014, 2.2177 ± 0.0014, and 2.1199 ± 0.0014 eV, respectively. The EA of *m*-methylenephenol was also obtained, 1.024 ± 0.008 eV. In all four cases, the dominant vibrational progressions observed are due to several ring distortion vibrational normal modes that were activated upon photodetachment, leading to vibrational progressions spaced by ~500 cm^{-1}. Using the methylphenol O-H bond dissociation energies reported by King *et al*. and revised by Karsili *et al.,* a thermodynamic cycle was constructed and the acidities of the methylphenol isomers were determined: $\Delta_{acid}H^0_{298\,K}$ = 348.39 ± 0.25, 348.~~13~~82 ± 0.25, 3~~48.87~~50.08 ± 0.25, and 349.~~26~~0 ± 0.25 kcal/mol for

cis-ortho-, trans-ortho-, m-, and *p*-methylphenol, respectively. The excitation energies for the ground doublet state to the lowest excited doublet state electronic transition in *o-, m-,* and *p*-methylphenoxyl were also measured: 1.029 ± 0.009, 0.962 ± 0.002, and 1.029 ± 0.009 eV, respectively. In the photoelectron spectra of the neutral excited states, C-O stretching modes were excited in addition to ring distortion modes. Electron autodetachment was observed in the cases of both *m*- and *p*-methylphenoxide, with the *para* isomer showing a lower photon energy onset for this phenomenon.

I. INTRODUCTION

Methylphenols, commonly referred to as cresols, are an important class of molecules in many fields of chemistry.[1-36] They are commonly used as model systems for hydrodeoxygenation in catalytic chemistry for refining biofuels,[2-6] while the internal rotations of the functional groups are of great interest to many spectroscopists.[7-13] Their thermochemistry and kinetics have also been studied, *e.g.* King *et al.*[26] measured the bond dissociation energies of the O-H bond in each isomer of methylphenol to high accuracy (± 0.14 kcal/mol), while McMahon and Kebarle[36] implemented proton-transfer equilibria studies to measure their gas phase acidities. The study of the thermochemistry of methylphenols is often motivated by the desire to understand the effect of different benzene substitutions on reactivity, particularly in comparison with their simpler counterparts, phenol and toluene. Through these comparisons, insight can be gained into the relative contribution of the OH group (which is strongly electron donating in aromatic systems) compared to the CH_3 group (weakly electron donating), and how these two functional groups work in concert to affect reactivity and electronic structure. Methylphenols have been extensively studied using a large variety of spectroscopic techniques, including microwave absorption,[7,9] Laser Induced Fluorescence (LIF),[8,10,11,13,21] Resonance Enhanced

Multiphoton Ionization (REMPI),[18,20,24] stimulated Raman-UV optical double resonance,[23] and Hole Burning spectroscopy. In addition to purely spectroscopic probes, these compounds have been ionized and detected using Time of Flight (TOF)[18,24] and Fourier-Transform Ion Cyclotron Resonance (FTICR) mass spectrometry.[35] However, very little experimental information on the methylphenoxyl radicals or their thermochemistry is available. Despite the numerous studies and the reliance on methylphenols as a model species in catalytic and combustion chemistry, the electron affinity (EA) of *p*-methylphenoxyl has only been measured to an accuracy of ~100 meV,[36] while there are no measurements for the other isomers, and the gas phase acidities of all three isomers have been measured with a fairly large uncertainty (at least 2 kcal/mol).

The present study uses photoelectron spectroscopy to determine accurate EAs of the methylphenoxyl radicals, and, in concert with quantum chemical calculations, provides physical insight into the structures of both the methylphenoxide anions and methylphenoxyl radicals. Combining the highly accurate (error of ± 0.14 kcal/mol) O-H bond dissociation energy for each methylphenol isomer from King *et al*.,[26] as modified by Karsili *et al.*,[37] with the EAs measured in this study allows for the construction of a thermodynamic cycle that provides accurate gas phase acidities.[34] The results will also be compared with the previous work on the phenoxide[38,39] and benzyl[39] anions, which were also studied using anion photoelectron spectroscopy. One might ask if the methylphenoxyls will display a combination of attributes previously shown by those two anions, or will the chemistry and spectroscopy have qualitatively different behavior? For example, one major difference between the *ortho, meta,* and *para* isomers of methylphenol is based on possible resonance structures, which will likely influence the derived chemical properties.

II. EXPERIMENTAL METHODS

Two unique instruments with complementary strengths are used to investigate the methylphenoxide anions and their corresponding radicals using anion photoelectron spectroscopy. The first instrument utilizes a single frequency cw argon ion laser light source and a constant spectral resolution hemispherical electron kinetic energy analyzer to measure photoelectron spectra. The second instrument is based on pulsed techniques, using a tunable nanosecond laser to photodetach electrons, and obtains the electron velocity distribution with a Velocity Map Imaging (VMI) photoelectron spectrometer, whose instrument resolution is a function of the kinetic energy of the electrons. The two instruments also differ in the mass resolution and ion generation techniques. In both experiments, methylphenol samples were obtained from Sigma Aldrich (≥ 98% purity) and used without further purification. Their chemical structure and chemical purity were verified with ^{1}H NMR.

The first of the two experimental instruments employed in this study has been described in detail previously,[40,41] and hence, only a brief description with an emphasis on the methylphenoxide anion production is provided. Methylphenoxide anions are prepared in a flowing afterglow (FA) ion source by proton abstraction from the parent methylphenol molecules using the hydroxide anion, OH^-, or the amide anion, NH_2^-, in approximately 0.5 Torr of helium (He) buffer gas. After the products (both ionic and neutral) are formed, they remain in the flow tube for several milliseconds, undergoing collisions with the helium carrier gas, the trace methylphenol reactant gas, and other products. The flow tube is cryogenically cooled to ~200 K. This collisional environment allows the reactants and products to evolve toward chemical equilibrium, so the detected anion products need not be the nascent deprotonated products. The dominant anion product observed corresponds to deprotonation of the most acidic site, with trace amounts of other products. Both OH^- and NH_2^- are energetically capable[42,43] of deprotonating either the hydroxyl or the methyl sites for all three isomers, although the hydroxyl site is

the most acidic site by over 30 kcal/mol (according to calculations at the B3LYP/aug-cc-pVQZ level, listed in the Supplementary Material). The NH_2^- anion is also energetically capable of deprotonating directly from the benzene ring, but this anion product channel is not observed.

At the end of the flow tube, the anions in the center of the flow pass through a 1-mm orifice into a differentially pumped chamber (~10^{-6} Torr). In this chamber, the ions are focused, steered, and accelerated to 735 eV, mass selected with a Wien velocity filter ($m/\Delta m \approx 60$), and then decelerated to 35 eV before entering the laser-anion interaction region. In the interaction region, the mass-selected anions are intersected by single frequency radiation (363.806 nm, 3.40814 eV) obtained from an Ar-Ion laser. A small solid angle of the photodetached electrons are collected in a direction perpendicular to the laser and ion beams. The kinetic energy of these electrons are then measured by a hemispherical energy analyzer with a constant electron energy resolution of 10 meV. Calibration of the absolute electron energy scale is achieved by measuring the $O(^3P_2) + e^- \leftarrow O^- (^2P_{3/2})$ transition in the atomic O^- photoelectron spectrum using the known EA of the O atom, 1.46112 eV.[44] Additionally, a small energy scale compression factor (0.7%) is applied based on the photoelectron spectrum of O_2^-, which is determined by comparing measured peak positions to the well-known photoelectron spectrum of O_2^-.[45] The photoelectron spectra reported here from this machine were obtained with the laser polarization oriented at the magic angle of 54.7° with respect to the photoelectron collection plane. This orientation yields photoelectron intensities that are proportional to the total photodetachment cross-section.[46] The laser polarization was scanned to measure the anisotropy in the photoelectron angular distribution, specifically for the peak corresponding to the origin transition in the methylphenoxide anion photoelectron spectra. For the methyl deprotonated product for the *meta* isomer, the reported anisotropy parameter was averaged across the spectrum.

The second apparatus has also been described in detail previously.[47] Briefly, the anions of interest are produced in a dual pulsed valve plasma entrainment source, again from the deprotonation of methylphenol by reaction with OH^-.[48] This source uses two separate pulsed General Valves set perpendicular to each other. One is designated the primary supersonic expansion (10 psig, ~1% methylphenol in Ar), while the other valve is designated the side valve (35 psig, 1% O_2, 30% H_2 balance Ar). Under normal operating conditions, the side valve tension is adjusted such that it is responsible for only ~10% of the total pressure rise in the vacuum chamber. The side valve also features a pulsed plate discharge at the valve exit (–2000 V),[48] generating a plasma which is then entrained in the primary supersonic expansion. The OH^- generated in the plasma source undergoes reactions with the methylphenol isomer of interest contained in the main expansion, generating products which are collisionally cooled with Ar. While not necessary to be the case, the most thermodynamically favorable products (methylphenoxide anions) were found to be by far the dominant deprotonated methylphenol produced.

Following the initial expansion, the anions are directed into a Wiley-McLaren TOF mass spectrometer by a pulsed extraction plate, where the ions are separated by their mass to charge ratio (m/z) and spatially focused in the center of a VMI interaction region.[49] An appropriately timed nanosecond laser pulse (discussed below) intersects the anion packet, photodetaching electrons. All of the photodetached electrons are velocity mapped onto a position sensitive phosphor screen-coupled microchannel plate detector, and subsequently imaged by a CCD camera. This photoelectron image is analyzed first by reconstructing the two dimensional image into a three dimensional velocity distribution using an inverse Abel transform as part of the BASEX program package. This three dimensional distribution is then converted to a one dimensional electron speed distribution, and finally an electron Kinetic Energy (eKE) distribution by a Jacobian transformation. This spectrum is converted to an

electron Binding Energy (eBE) distribution by subtracting ~~the~~ eKE from the laser photon energy, yielding the reported photoelectron spectra. For these experiments, the energy scale is calibrated by the S^- photoelectron spectrum.[50,51]

In contrast with the hemispherical analyzer, the VMI spectrometer has a spectral resolution that is a function of eKE, namely the resolution decreases with increasing eKE. This resolution is determined by the eKE and the Full Width at Half Maximum (FWHM) of a peak in a photoelectron spectrum due to a single transition. In this case, an atomic anion (S^-) was used to determine the resolution as a function of electron kinetic energy, as well as calibrate the energy scale. Typically, the resolution is ~2–3% (resolution ~ FWHM/eKE). However, if the photon energy is within ~50 meV of the binding energy of a transition, this results in low kinetic energy electrons, and the instrument attains a resolution of ~3 meV. This technique is commonly referred to as Slow Electron Velocity Map Imaging (SEVI).[52] To take advantage of the varying energy resolution of this spectrometer, a variety of photon energies are used in this experiment. The 3rd harmonic of a nanosecond Nd:YAG laser is used directly (355 nm, 3.494 eV). In addition, a visible light OPO is pumped by the 3rd harmonic of the Nd:YAG laser, supplying tunable light between 400 and 600 nm. Finally, the second harmonic of the Nd:YAG laser (532 nm, 2.330 eV) is used to pump a dye laser using DCM dye and producing 647 nm light, which is then frequency doubled to produce 323 nm (3.832 eV) light.

III. THEORETICAL METHODS

Electronic and vibrational quantum calculations were carried out using the Gaussian 09 program package.[53] All ground electronic state calculations were at the B3LYP/aug-cc-pVQZ level, which has been shown to be an effective compromise between accuracy and computational cost for large molecules, such as the substituted aromatic compounds studied here.[54] For excited electronic state

calculations, Time Dependent Density Functional Theory (TD–DFT) was used with the B3LYP functional and Dunning's correlation consistent basis set, aug-cc-pVTZ. The energies and geometries of the anion ground electronic states, neutral ground electronic states, and neutral first excited electronic states were optimized for all isomers. In the case of each isomer, the ground and excited electronic state vibrational information was calculated separately for every anionic and neutral state used to simulate the PE spectra. In addition, the electron affinities (EAs) and electronic term energies for the *o-, m-*, and *p-* methylphenoxyl radicals were calculated. The calculated geometries, normal mode vectors, and the harmonic vibrational frequencies of the anion and the corresponding neutral are used to calculate the Franck-Condon (FC) factors for the simulated photoelectron spectra using the PESCAL program.[55] In addition, a Boltzmann distribution of anion internal energy is applied (150 K or 200 K for the pulsed and continuous experiments, respectively). In the simulation, the FC factors are calculated using the harmonic oscillator approximation, which includes Duschinsky rotations and employs the Sharp-Rosenstock-Chen method.[56-58] The calculated FC factors are shown as purple sticks in Fig. 2, 3, 4, 5, and 6. These sticks are then convolved with Gaussian functions, whose integral is normalized to be equal to the calculated transition intensity, and whose FWHM is consistent with instrumental resolution, which is a function of eKE for the VMI spectrometer and is a constant 10 meV for the hemispherical analyzer. The sum of these Gaussian functions results in the simulated spectra shown as green traces, which ~~has~~ have been scaled in each case to match the experimental peak amplitude of the origin transition. Each simulated spectrum has also been shifted by ~40–50 meV to match the experimental electronic band origin.

IV. RESULTS

Before scrutinizing the photoelectron spectra of the product anions generated from reacting OH^- (or NH_2^- in the FA source) with the methylphenol isomers, it is useful to consider how the resulting

photoelectron spectra from different deprotonated products might qualitatively vary. For example, the EA of the corresponding neutral is a good indication of where the methylphenol was deprotonated. If the product anion is the result of deprotonating the alcohol group, the electron affinity of the neutral should be similar to that of the phenoxyl radical (EA = 2.2538 ± 0.0008 eV[38]). If the product anion is instead the result of CH_3 deprotonation, it is reasonable to expect an EA of the corresponding neutral to be near that of the benzyl radical (EA = 0.912 ± 0.006 eV[39]). In either case, the electron is likely to localize on the deprotonated group; this should result in both a lengthening of the bond between the deprotonated group and the aromatic ring, as well as an elongation of the ring away from the negative charge when compared to the equilibrium geometry of the corresponding neutral radical. Thus, upon photodetachment, it might be expected that there will be vibrational transitions involving excitation in the neutral ring distortion modes with vibrational frequencies of ~ 500 cm^{-1}. In addition, it is reasonable to predict excitation of vibrational modes in the neutral that incorporate a stretching motion along the bond between the ring and the deprotonated group, which would have fundamental vibrational frequencies of ~ 1000 - 1500 cm^{-1}. In the rest of this section, the resulting EAs, neutral term energies, and vibrational analysis derived from the observed photoelectron spectra will be summarized. For each photoelectron spectrum, the vibrational analysis is performed by comparing the observed spectrum with the calculated photoelectron spectrum simulation. Throughout this work, the error in the reported peak positions are related to the statistical error in finding the peak center, the error in the absolute energy scale, and the number of independent measurements of particular peaks. When reporting the position of a particular transition, such as the neutral vibrational frequencies or the EA, this error is combined with the error associated with the offset of the actual transition from the peak center. This uncertainty can be near zero if only a single transition is the major contributor to the peak shape, or, if there are multiple transitions under the peak envelope, it could be as much as the Half-Width-at-Half-Maximum (HWHM)

of the peak. Note that the peaks presented in the reported spectra are broader than the instrument resolution and always arise from multiple transitions, so this latter error dominates the reported uncertainty. In the error analysis for each isomer, rotational contours were also considered. In every case, the analysis of Engelking was used[59] and in all cases the shift between peak centers of a particular transition and the true origin were estimated to be less than 0.1 meV. Thus this effect was accounted for in the uncertainty of the measurements contained in this work, but was determined to have a small impact on the reported error, even in the case of the EA measurements.

A. Electron Affinities and Term Energies of Methylphenoxyl Radicals

In order to gain an overview of the full photoelectron spectra, data were collected on the VMI spectrometer with a photon energy of 3.494 eV (Fig. 1). Following deprotonation from all three reactant isomers (*o*-, *m*-, and *p*-methylphenol), there are two progressions observed. The first progression begins at approximately 2 eV eBE, with a second progression appearing at ~ 3 eV eBE. Considering the prior arguments, this would suggest that the anionic product formed is indeed methylphenoxide for all three reactant isomers. Further, considering the photoelectron spectroscopy spin selection rule $\Delta S \pm ½$, and the fact that the methylphenoxide anion electronic ground state has singlet spin multiplicity, these two observed progressions must both be of doublet multiplicity. The progression starting near 2 eV in binding energy for each isomer arises from electron detachment from the anion singlet ground electronic state to form the neutral doublet ground electronic state (labeled $\tilde{X}$). Each progression starting near 3 eV in binding energy corresponds to a vibrational progression arising from transitions from the anion singlet ground electronic state to the first excited doublet electronic state of the neutral (labeled $\tilde{A}$) of methylphenoxide. These assignments will be justified in the following paragraphs. While all three isomers of methylphenol show evidence of methylphenoxide products, another progression starting near 1 eV is observed for only the *meta* isomer. This will be shown to be the photoelectron spectrum of the

anion product arising from the deprotonation of the methyl group (see Section E), forming the methylenephenol radical. It is not expected, based on TD-DFT calculations, that excited states of methylenephenol would be energetically accessible in this study.

High resolution photoelectron spectra of the origin peaks for the transition to the neutral $\tilde{X}$ state for each of the three methylphenoxide isomers were obtained using the SEVI technique (Fig. 2). In addition to measuring these portions of the spectra with increased resolution, the photoelectron spectra were also simulated and overlaid with experimental data. Considering the excellent agreement between the experiment and simulation, we report the EA of *o-, m-,* and *p*-methylphenoxyl as 2.1991 ± 0.0014, 2.2177 ± 0.0014, and 2.1199 ± 0.0014 eV, respectively (summarized in Table I).

The transition to the neutral $\tilde{A}$ state was investigated for all three isomers making use of 3.494 eV photons with the VMI spectrometer and shown in Fig. 3. The photoelectron spectra for this transition were simulated and overlaid with the experimental data, and again, these agree very well. Therefore, we can identify the electronic band origin of these progressions at 3.228 ± 0.009, 3.180 ± 0.002, and 3.149 ± 0.009 eV electron binding energy for *o-, m-,* and *p*-methylphenoxyl, respectively. Thus the term energy between the ground and first excited doublet electronic states of the neutral radicals are determined: 1.029 ± 0.009, 0.962 ± 0.002, and 1.029 ± 0.009 eV for *o-, m-,* and *p*-methylphenoxyl, respectively (summarized in Table I). This energy is very similar to that in phenoxyl (1.06(5) eV),[39] although the excited neutral state was not explored in detail in that study. Note that for the *ortho* and *para* isomers, a conservative error bar of 9 meV is used. This is based on the HWHM of the origin peak. However, the simulation suggests that for the *meta* isomer, less significant transitions are symmetrically distributed about the origin transition in peak A, suggesting that a smaller error bar of ± 0.002 eV is warranted.

In addition to the electron affinities, photoelectron angular distributions with respect to the laser polarization, characterized by the anisotropy parameter (β), were measured for these photoelectron spectra.[46] Since the electron is being detached from what can be described as an oxygen p-like orbital, it is expected that we should observe a negative β. Photodetachment forming the neutral $\tilde{X}$ state shows the same photoelectron anisotropy for the three isomers, β ~ – 0.3, using 3.494 or 3.408 eV photons. This was also measured for the methylenephenol anion, and is approximately the same as for the methylphenoxides, β ~ – 0.3. The photoelectron angular distribution resulting from photodetachment to form the neutral $\tilde{A}$ state for all three isomers were isotropic (β ~ 0). However, these transitions are all close in binding energy (< 400 meV) to the photon energy used to examine them, and so an isotropic angular distribution is expected.[60]

B. Vibrational Analysis: *ortho*-Methylphenoxyl

The vibrational progression in the *o*-methylphenoxide photoelectron spectrum resulting from the transition to the *o*-methylphenoxyl radical $\tilde{X}$ state was studied in the hemispherical analyzer and is shown in Fig. 4. It is evident that there is a progression resulting from exciting ring distortion vibrational modes, as the dominant peaks observed are spaced by approximately 500 cm^{-1}, as expected. All of the observed peaks are broader than the instrument resolution, implying that each peak is comprised of multiple overlapping transitions. Nonetheless, the partially resolved peak doublet labeled B and C may be fit to two Gaussian functions, and their positions relative to the band origin are 434 ± 8 and 542 ± 8 cm^{-1}, respectively. While all of the peaks with larger binding energy than C are predicted to be due to multiple transitions and are beyond the ability of either instrument to resolve, peaks B and C are predicted to be primarily due to only a few transitions. Peak B is predicted to be due to a transition from the ground vibrational state of the anion to one quanta in a ring distortion vibrational mode in the neutral (33_0^1 = 430 ± 80 cm^{-1}), which has a calculated harmonic frequency of 453 cm^{-1}. Peak C is due to two

transitions, each starting in the ground vibrational state of the anion and going to one quanta in two different ring distortion vibrational modes of the neutral molecule (30_0^1, 31_0^1 = 540 ± 80 cm^{-1}). These two modes are calculated to have harmonic frequencies of 540 and 577 cm^{-1}. The hindered methyl rotor vibrational mode was possibly resolved for *o*-methylphenoxyl, seen in Fig. 2, indicated with an asterisk, and located 196 ± 8 cm^{-1} relative to the origin. This peak is likely due to a transition from the ground vibrational state in the anion to two quanta in the hindered methyl rotor vibration in the neutral state, 39_0^2 = 196 ± 16 cm^{-1}. Neglecting anharmonicity, 39_0^1 = 98 ± 8 cm^{-1} is derived, which compares well with the calculated harmonic frequency of 106 cm^{-1}. However, due to the inherent complexity of hindered rotor vibrations, a harmonic approximation is likely not valid, and so this assignment, while plausible, is only suggested.

The vibrational progression resulting from the transition to the excited electronic $\tilde{A}$ state of the *o*-methylphenoxyl radical can be seen in Fig. 3. None of the peaks observed in the spectrum are resolution limited, which again indicates that there are multiple transitions contributing to each peak. The photoelectron spectrum was simulated and reproduces the experiment with excellent agreement. Peak A is assigned as the band origin, with peaks B and C being located 483 ± 16 cm^{-1} and 1225 ± 16 cm^{-1} higher in binding energy, respectively. While there are several predicted transitions with significant FC factors attributed to peak B, the peak intensity and position is primarily due to a transition from the anion vibrational ground state to one quanta in a ring distortion vibrational mode in the neutral $\tilde{A}$ state, 32_0^1 = 480 ± 190 cm^{-1}, predicted to have a harmonic frequency of 506 cm^{-1}. Peak C is similarly broadened past the instrument resolution, but its dominant contributor (based on FC factor intensity) is predicted to be due to a transition from the anion vibrational ground state to a single quanta in a quasi C–O stretching mode in the neutral $\tilde{A}$ state, 15_0^1 = 1220 ± 130 cm^{-1}, predicted to have a harmonic frequency of 1312 cm^{-1}.

C. Vibrational Analysis: *meta*-Methylphenoxyl

The vibrational progression in the *m*-methylphenoxide photoelectron spectrum resulting from detachment to the *m*-methylphenoxyl radical $\tilde{X}$ state was studied in the continuous experiment (see Fig. 4). As with the *ortho* isomer, a progression spaced by approximately 500 cm^{-1} is observed for the *meta* isomer, once again suggesting that ring distortion modes are excited upon photodetachment of the anion. Assuming that peaks B–D are due to only one mode, these peaks are due to transitions from the ground anionic state to 1, 2, or 3 quanta of a single vibrational mode in the neutral state, with peak locations (relative to the EA) of 564 ± 8 cm^{-1}, 1079 ± 8 cm^{-1}, and 1587 ± 8 cm^{-1} for peaks B, C, and D, respectively. These correspond to the following transitions: 31_0^1 = 560 ± 50 cm^{-1}, 31_0^2 = 1080 ± 64 cm^{-1}, 31_0^3 = 1590 ± 90 cm^{-1}. The simulated spectr~~a~~um (overlaid) agrees well with the experiment and confirms that this vibrational progression is primarily due to transitions from the ground anionic state to excitation in a ring distortion vibrational mode in the neutral state with a calculated harmonic frequency of 540 cm^{-1}, agreeing with the experimentally measured 31_0^1 = 560 ± 50 cm^{-1} transition. The hindered methyl rotor vibrational mode was also likely measured for *m*-methylphenoxyl (Fig. 2, designated with an asterisk, located at 134 ± 8 cm^{-1} relative to the origin). This peak is possibly due to a transition from the ground vibrational state in the anion to two quanta in the hindered methyl rotor, 39_0^2 = 135 ± 16 cm^{-1}. This allows for a determination of the methyl hindered rotation vibrational frequency, assuming no anharmonicity, 39_0^1 = 67 ± 8 cm^{-1}, compared with the calculated harmonic frequency of 81 cm^{-1}. Again, this assignment should only be suggested, due to the anharmonicity of hindered rotor vibrations.

The photoelectron spectrum vibrational progression observed for the transition to the excited $\tilde{A}$ state of the *m*-methylphenoxyl radical can be seen in Fig. 3, overlaid with the simulated spectrum. Peak A is assigned as the band origin, with peaks B and C located 523 ± 8 cm^{-1} and 1260 ± 8 cm^{-1} higher in binding energy, relative to peak A. According to the simulation, peak B has many contributing

transitions, broadening it past instrument resolution, but it is primarily due to two transitions from the anionic ground vibronic state to one quanta in either of two ring distortion vibrational modes in the neutral $\tilde{A}$ state, 31_0^1, 32_0^1 = 520 ± 96 cm^{-1}, predicted to have harmonic frequencies of 516 and 542 cm^{-1}. These peaks cannot be resolved due to our instrument resolution. Peak C is similarly broadened past instrument resolution and is predicted to be primarily due to a transition from the anionic ground state to a single quanta in a quasi O–C stretching mode in the neutral $\tilde{A}$ state, 15_0^1 = 1260 ± 90 cm^{-1}, which has a calculated harmonic frequency of 1330 cm^{-1}.

D. Vibrational Analysis: *para*-Methylphenoxyl

The photoelectron spectrum of *p*-methylphenoxide, accessing the neutral $\tilde{X}$ state, was studied in the VMI spectrometer with a photon energy of 2.520 eV (Fig. 4). Peak A is assigned as the band origin. Peaks B and C, located at 460 ± 8 cm^{-1} and 921 ± 8 cm^{-1} relative to the origin, suggest a vibrational progression arising from transitions from the ground state of the anion to the *p*-methylphenoxyl ground state with one or two quanta (for peaks B and C) in a ring distortion vibrational mode in the neutral radical, 32_0^1 = 460 ± 40 cm^{-1} and 32_0^2 = 920 ± 40 cm^{-1}. The simulated spectrum agrees with the measured transition, and predicts this ring distortion harmonic frequency to be 463 cm^{-1}. There is one notable disagreement with theory that may be seen in this spectrum, located at ~2.5 eV binding energy and labeled D. Peak D contains 3 separate peaks at 2893 ± 8, 2931 ± 8, and 3006 ± 8 cm^{-1}, relative to peak A. These are reasonable frequencies for C-H stretching modes in the radical, but their intensities are not recovered in the simulation. It should be noted that due to the nature of the variable resolution of the VMI and the location of the peaks being close to the photon energy, the peak amplitudes exaggerate the perceived importance of these transitions. In fact, the integrated intensity of these peaks are approximately equal to half the intensity of peak C.

The *p*-methylphenoxide photoelectron spectrum accessing the neutral excited $\tilde{A}$ state is shown in Fig. 3, and overlaid with the simulated spectrum. Peak A is the band origin. Peak B, located 459 ± 8 cm^{-1} from the origin, corresponds to the transition from the anionic vibrational ground state to one quanta in a ring distortion vibrational mode in the neutral $\tilde{A}$ state, 32_0^1 = 460 ± 80 cm^{-1}, with a predicted harmonic vibrational frequency of 461 cm^{-1}. Peak C, located at 1239 ± 8 cm^{-1} relative to the origin, is assigned to a transition from the anionic ground vibrational state to one quanta in a quasi C–O stretch vibrational mode, 15_0^1 = 1240 ± 90 cm^{-1}, in the neutral $\tilde{A}$ state with a calculated fundamental vibrational frequency of 1320 cm^{-1}. Finally peak D, located at 1703 ± 80 cm^{-1}, relative to peak A, is assigned to a combination band, $15_0^1 32_0^1$ = 1700 ± 90 cm^{-1}.

E. CH_3 Deprotonated *meta*-Methylphenol

The *meta* isomer of methylphenol behaves differently from the other isomers in its chemical reactivity. While the other isomers only show evidence of deprotonation at the alcohol group, the *meta* isomer displays deprotonation at the methyl group as well. The photoelectron spectrum of methyl deprotonated *m*-methylphenol is shown in Fig. 5, with the simulated spectrum overlaid. While the agreement between the experiment and the simulation is clear, there is more broadening than predicted. The dominant peaks in the spectrum are spaced by ~500 cm^{-1}, again indicating that there is significant vibrational activity in ring distortion vibrational modes in the neutral radical. Peak A, the band origin, arises from the transition from the ground vibronic state of the anion to the ground vibronic state of the neutral. As such, the EA of *m*-methylenephenol is 1.024 ± 0.008 eV. Peak B is located 513 ± 8 cm^{-1} higher in binding energy relative to peak A. The simulation predicts that peak B is mainly due to vibrational transitions from the anionic ground state to one quanta in either of two modes, 31_0^1, 30_0^1 = 510 ± 110 cm^{-1}, with predicted harmonic frequencies of 525 and 547 cm^{-1}. However, due to our resolution, we could not resolve these. Our calculations show that the CH_2 and OH groups lie in the

plane of the ring for both anion and neutral states, and thus excitations of CH_2 umbrella modes or OH internal rotations are neither expected nor observed.

F. Photon Energy Dependence of the *para*-Methylphenoxide Photoelectron Spectra

The photoelectron spectrum of *p*-methylphenoxide was first obtained using the fixed frequency (364 nm, 3.408 eV) spectrometer. The simulated spectrum did not reproduce the relative intensity of the first three peaks in the experimental photoelectron spectrum as well as we would normally expect; additionally, empirically adjusting bond lengths and angles did not improve the comparison. Consequently, the VMI instrument, which utilizes a tunable light source, was employed to reinvestigate the photoelectron spectrum of *p*-methylphenoxide at a number of photon energies above and below 3.408 eV, and shown in Fig. 6. The photon energies employed spanned from 3.494 eV (panel **A**) to 2.520 eV (panel **D**). The experimental photoelectron spectra show substantial variations over this range of photon energies. An additional two photon energies were used during this investigation and are reported in the Supplementary Material.

An important assumption for all of the calculated photoelectron spectra simulations reported here is that the electronic contribution to the overall photodetachment cross section is essentially constant over the photon energy range corresponding to the width of the vibronic envelope; in this limit, the relative intensities of the vibronic transitions are well-represented by the calculated Franck-Condon factors. This assumption means that the simulated photoelectron spectrum should not depend on photon energy. Thus the photoelectron spectra simulations (solid green lines) plotted in all four panels of Fig. 6 differ only in the convolution of the Franck-Condon factors to reflect the changing experimental resolution with photoelectron kinetic energy. The experimental data in Fig. 6, however, show a significant photon energy dependence of the *p*-methylphenoxide photoelectron spectrum, which cannot

be justified by the changing experimental resolution. While there is good agreement between the experiment and the photoelectron simulation at the lowest photon energy (panel **D**), theory and experiment fall further out of agreement as the photon energy increases. As the photon energy is increased, there are several peaks which change intensity relative to the origin peak, and there is an appearance of a broad continuum under the spectrum in the top panel. For example, the highlighted peak in Fig. 6 changes intensity relative to its neighboring peaks with different photon energies. This behavior arises from electron autodetachment, a multistep process whereby the anion absorbs a photon to an excited *anionic* state which lies above the electron detachment threshold, and subsequently transfers to the *neutral* ground electronic state, ejecting an electron in the process. TD-DFT calculations predict eight optically accessible anion excited electronic states between 1.9 and 3.3 eV above the ground anion state, and thus it is outside the scope of this work to further pursue a theoretical modeling of these spectra. In the current study, *m*-methylphenoxide also displayed evidence of autodetachment, but at a greater photon energy (3.832 eV) than *p*-methylphenoxide. (See Fig. S3 in Supplementary Material.) Observing autodetachment from *o*-methylphenoxide was not pursued in this work, but likely exists as well. This will be discussed in greater detail in the following section.

V. DISCUSSION

The photoelectron spectra of methyl deprotonated *m*-methylphenol and *o-, m-,* and *p*-methylphenoxide have been presented. In the following discussion, the electron affinities and active vibrational modes of the corresponding neutral radicals will be compared with other substituted aromatic radicals, *e.g.* halobenzyl, phenoxyl, and benzyl radicals. In addition, the autodetachment behavior of the methylphenoxides studied in this work will be discussed and compared with previous work on

phenoxide. Finally, we combine the experimental EAs with the methylphenol O–H bond dissociation energies[26,37] ~~measured by King *et al.*[26]~~ to derive the gas phase acidity of the three methylphenols.

The electron affinities of the three methylphenoxyl isomers are all close to 2.2 eV, while the *meta* isomer has the largest EA, and the *para* has the smallest (see Table I). This ordering can be readily rationalized using resonance stabilization and aromaticity concepts: the *meta* isomer does not benefit from resonance stabilization of the neutral radical, whereas the *ortho* and *para* isomers do. In the neutral *meta* form, the electron donating group (CH_3) cannot donate charge to the strongly electron withdrawing O radical group, hence raising its energy relative to that of the other neutral isomers. For all three isomers, the anionic form is closed shell and would be minimally perturbed by resonance stabilization since there is a formal negative charge on O. Thus, it is the neutral resonance stabilization (or lack thereof in the *meta* isomer) that dictates the relative EA of the *meta* isomer compared to the *ortho* and *para* isomers. The relative EAs of the *ortho* and *para* isomers are more difficult to predict and explain the observed trend. Both benefit from resonance, and the *ortho* isomer has the additional complication of the O…CH_3 interaction. Regardless, it is experimentally determined that the *para* isomer has the lowest EA, while *meta* has the highest. This same trend is seen in the halobenzyls, which are also doubly substituted benzenes, but with an electron withdrawing group (CH_2) and another very weak electron withdrawing group (the halogens, by induction).[61]

There is only one prior experimental measurement of the EA of any of the methylphenoxyls in the literature. McMahon and Kebarle[36] used gas phase proton transfer equilibria to determine an EA for *p*-methylphenoxyl of ~2.17 eV. This result is consistent with our more accurate measurement of 2.1199±0.0014 eV. In addition to the previous experimental work, there was also a theoretical study by Angel and Ervin[27] which used CBS-QB3 calculations to ob~~s~~tain the EA of *m*-methylphenoxyl to be 2.19 eV. This calculation also agrees well with our experimental measurement of 2.2177±0.0014 eV.

The vibrational progressions seen in the photoelectron spectra for all of these molecules show the clear signature of both active ring distortion normal modes (for transitions to the neutral $\tilde{X}$ and $\tilde{A}$ states) and active quasi C–O stretching normal modes (for transitions to the neutral $\tilde{A}$ state). A summary of the measured (and calculated) vibrational frequencies for all three methylphenoxyl radicals is found in Table II. While many transitions comprise the spectra presented in this work, the transitions shown in this table account for all significant vibrational modes which compose the observed progressions for each isomer. As mentioned previously, this behavior can be explained with a simple physical picture. For the methylphenoxide anions, adding the extra electron elongates the bond between the oxygen and the aromatic ring, as well as elongating the bonds within the ring away from the localized negative charge on the oxygen, compared to the equilibrium structure of the neutral radical. Upon photodetachment, one would therefore expect the excitation of ring distortion vibrations, which are observed, and C–O stretches. However, there is little evidence for any significant activity in C–O stretching modes for the transition to the neutral $\tilde{X}$ state, and B3LYP calculations also predict little change in the C–O bond lengths. A similar physical picture can be obtained for the methyl deprotonated *m*-methylphenol photoelectron spectrum. For the photoelectron spectra of methylphenoxide accessing the neutral $\tilde{A}$ state, both ring distortion and C-O stretching modes are excited. The neutral $\tilde{A}$ state is formed by removing an electron from the aromatic π system in the anion, resulting in the π* neutral excited $\tilde{A}$ state. The antibonding π system in the benzene ring elongates the C-O bond length in the $\tilde{A}_{\text{neutral}}$ state relative to the anion. Thus, upon photodetachment from the anion to form the neutral excited $\tilde{A}$ state, one would expect this C-O stretching vibration to be active.

Beyond the direct comparison with previous studies of the methylphenoxyl radicals, similar substituted aromatic compounds should be considered. Perhaps the most obvious of this group would be phenoxyl and benzyl. The phenoxyl radical has an EA of 2.2538 ± 0.0008 eV.[38] There is a relatively

small decrease (< 130 meV) in the EA of phenoxyl upon the addition of a methyl group, forming the methylphenoxyl radicals studies here. Methyl is a very weak electron donating group and so it is expected to have only a minor effect on the EA. It was observed that phenoxide had the same ring distortion vibrational modes excited upon photodetachment as are seen here for all three of the methylphenoxides.

In the case of deprotonation from the methyl group, a comparison with benzyl is appropriate. The EA of benzyl is 0.912 ± 0.006 eV.[39] Benzyl shows a minor increase (~0.1 eV) in its EA upon attaching a *meta* hydroxyl group, forming methylenephenol radical. This is perhaps surprising considering OH is a strongly electron donating group in aromatic systems, and therefore might lead one to conclude that it should largely disrupt the electronic structure of the system and thus the EA. However, there are two reasons why this is actually not the case. First, the only isomer of methyl deprotonated methylphenol observed in this work is the *meta* isomer. *Meta* isomers in aromatic systems are unique for their lack of resonance structures compared to that of *ortho* and *para* isomers. Hence, the impact of the electron donating effect of the OH in the *meta* isomer is diminished. Second, the primary effect of adding an electron donating group to the aromatic ring would be to localize the negative charge in the CH_2 carbanion. However, the charge is already localized on the CH_2 group, hence the change in overall behavior would be minimal. Both *m*-methylenephenol and benzyl show similar ring distortion vibrational progressions in their photoelectron spectra, further confirming the low level of perturbation.

In addition to comparing the EAs and vibronic structure of methylphenoxyl radicals, the methylphenoxide anion autodetachment behavior can be compared and discussed. Gunion *et al.*[39] and more recently Liu *et al.*[62] found autodetachment in the photoelectron spectroscopy of phenoxide. Specifically Liu *et al.* identified a dipole bound anion electronic excited state as the state responsible for facilitating autodetachment. Hydroxyphenoxide, a close analog of methylphenoxide, has also been

recently studied.[63,64] Autodetachment was observed in the photoelectron spectrum of *o*-hydroxyphenoxide, again attributed to a dipole bound anion electronic excited state.[63] In the current study, the *m*- and *p*-methylphenoxide anions both display signatures of electron autodetachment. Considering the many similarities between the methylphenoxides, one might also expect to observe autodetachment in the *ortho* isomer, but this was not pursued experimentally in this work. For *m*-methylphenoxide (see Supplementary Material for more information), there is a higher onset energy (3.494 eV< $h\nu_{onset} \leq$ 3.832 eV) for observing autodetachment as compared to the *para* isomer (2.520 eV< $h\nu_{onset} \leq$ 2.637 eV). These onsets and the anion state(s) involved could not be confirmed by our TD-DFT anion excited state calculations, primarily due to the abundance of available predicted excited electronic states that could be responsible for this phenomenon. The TD-DFT calculations suggest a similar number of optically accessible excited states for all three anionic isomers. However, theoretically investigating this further is beyond the scope of this work.

Having measured the electron affinities of the methylphenoxyl radicals, these results are combined with the measured bond dissociation energies[26,37] ~~obtained by King *et al.*[26]~~ (Table I) to determine the gas phase acidities using a thermodynamic cycle.[34] This cycle provides a direct experimental measure of the 0 K enthalpy with a small (± 0.14 kcal/mol) uncertainty for the deprotonation reaction: HA → $H^+ + A^-$. The dominant source of uncertainty arises from the error associated with the H–A bond strength, as seen in Table I. We may further combine this 0 K result with the calculated constant pressure heat capacities of the species involved in the acid reaction in order to obtain the enthalpy at 298 K:[34]

$$\Delta_{acid}H^0_{298\,K}(\mathrm{CH_3PhOH}) = \Delta_{acid}H^0_{0K}(\mathrm{CH_3PhOH}) + \int_0^{298}\left[C_p(\mathrm{CH_3PhO^-}) + C_p\,(H^+) - C_p(\mathrm{CH_3PhOH})\right]dT$$

This results in $\Delta_{acid}H^{0}_{298\,K}$ = 348.39 ± 0.25, 348.~~13~~82 ± 0.25, 3~~48.87~~50.08 ± 0.25, and 349.~~26~~0 ± 0.25 kcal/mol for *cis-ortho-, trans-ortho-, m-,* and *p*-methylphenol, using a conservative estimate of the error associated with calculating the C_p of these various molecules.[34] These results are also found in Table I. Note that King *et al*.[26] were able to differentiate between *cis-ortho* and *trans-ortho* isomers of methylphenol, where *cis* and *trans* refer to the direction of the hydrogen of the OH group with respect to the CH_3 group.

The acidities of the three methylphenol isomers (four isomers, if the *cis-,* and *trans-* conformers of the *ortho* isomer are considered) have been studied several times in the past. In general, the reported error bars have been in the range of 1-3 kcal/mol. McMahon and Kebarle[36] initially measured the acidity at 298 K of *o*-methylphenol as 346.2 kcal/mol. Two other studies (McMahon *et al.* [36] and Angel *et al.*[27]) examined *m*-methylphenol and determined the gas phase acidity at 298 K to be 347.3 and 348.2 ± 1.2 kcal/mol, respectively. Finally, *p*-methylphenol was studied by McMahon[36] and determined the gas phase acidity at 298 K to be 347.7 kcal/mol. The current study presented here agrees well with the previous studies, and has greatly improved on these measurements with an error of ± 0.25 kcal/mol. In addition to a direct comparison, one could also compare the acidity of phenol at 298 K (348.0 ± 1.0 kcal/mol, reported by Angel and Ervin,[27] or the 0 K acidity derived from the works of Kim *et al*.[38] and King *et al*.[65]: 347.43 ± 0.12 kcal/mol) to that of the methylphenols. The addition of a methyl group to a phenol minimally affects the acidity by increasing the room temperature reaction enthalpy by only ~ 1 kcal/mol. It is interesting, though, that because of the increased accuracy in the current study, one is able to observe that the trend in acidity increases going from *ortho* to *para* isomers. This order is due to the combination of the D_0 and the EA measured for each isomer; the trend is not mirrored in the D_0 and EA energetic ordering, where increasing D_0 and EA goes as *para*, *ortho*, *meta* instead. This order is also

different than that observed for the aqueous acidity, which places the trend *ortho, para, meta* for increasing acidity,[66] likely due to solvation effects.

VI. CONCLUSION

The EAs of *o-, m-,* and *p*-methylphenoxide were measured: 2.1991±0.0014, 2.2177±0.0014, and 2.1199±0.0014 eV, respectively. The EA of *m*-methylenephenol was also measured: 1.024 ± 0.008 eV. Using the methylphenol (O-H) bond strengths reported by King *et al.*[26] and revised by Karsili *et al.*[37] a thermodynamic cycle was constructed and the acidities of the three methylphenols were obtained to a substantially degree of accuracy than previously reported, with $\Delta_{acid}H^0_{298\,K}$ = 348.39 ± 0.25, 348.~~13~~82 ± 0.25, 3~~48.87~~50.08 ± 0.25, and 349.~~26~~0 ± 0.25 kcal/mol for *cis-ortho-, trans-ortho-, m-,* and *p*-methylphenol. The term energies for the neutral $\tilde{A} \leftarrow \tilde{X}$ doublet π to doublet π* transition in the three isomers of methylphenoxyl were measured: 1.029 ± 0.009, 0.962 ± 0.002, and 1.029±0.009 eV, for *ortho*, *meta*, and *para* isomers, respectively. In all reported photoelectron spectra, ring distortion vibrational normal modes were activated upon photodetachment, leading to vibrational progressions spaced by ~500 cm^{-1}. For the photoelectron detachment to the neutral $\tilde{A}$ states, C–O stretching modes were also excited, leading to additional vibrational transitions with associated frequencies of ~ 1300 cm^{-1}. Electron autodetachment was observed in both *m*- and *p*-methylphenoxide photoelectron spectra, although the *para* isomer had an earlier onset photon energy for observing autodetachment, despite having similar calculated anion excited electronic states.

SUPPLEMENTARY MATERIAL

See supplementary material for additional photoelectron spectra, additional details on gas phase acidity calculations, and illustrations of the Franck-Condon active normal modes discussed in the text.

ACKNOWLEDGEMENTS

W.C.L gratefully acknowledges support from NSF (Grants PHY1125844 and CHE1213862) and AFOSR (Grant FA9550-12-1-0125) for significant contributions to this project. The authors also thank Professor Bob McMahon (University of Wisconsin – Madison) for his early insights into the complexities in the *p*-methylphenoxide photoelectron spectrum.

TABLE I. Summary of results. The SEVI technique was used to obtain the EAs of the three methylphenoxyl isomers. Combining these with the results from King *et al.*[26] and Karsili *et al.*[37] allows for the determination of the gas phase acidities shown. The term energies determined in the current study for the methylphenoxyl radical $\tilde{A} \leftarrow \tilde{X}$ electronic transitions are also listed.

Deprotonated Methylphenol Isomer	EA (eV)	$D_{0,0K}$ (CH_3-PhO-H) (kcal/mol)[a]	$\Delta_{acid}H^o_{0K}$ (CH_3-PhO-H) (kcal/mol)	$\Delta_{acid}H^o_{298K}$ (CH_3-PhO-H) (kcal/mol)[b]	T_0 ($\tilde{A} \leftarrow \tilde{X}$) ($CH_3$-PhO$^\bullet$) (eV)
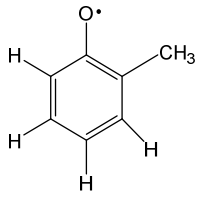	2.1991 ± 0.0014	*cis* 84.43 ± 0.14 *trans* 84.~~17~~86 ± 0.14	*cis* 347.31 ± 0.14 *trans* 347.~~05~~74 ± 0.14	*cis* 348.39 ± 0.25 *trans* 348.~~13~~82 ± 0.25	1.029 ± 0.009
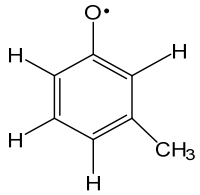	2.2177 ± 0.0014	8~~5.33~~6.53 ± 0.14	34~~7.77~~8.98 ± 0.14	3~~48.87~~50.08 ± 0.25	0.962 ± 0.002
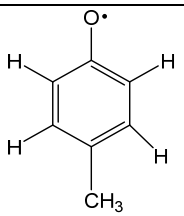	2.1199 ± 0.0014	83.~~43~~83 ± 0.14	348.~~13~~53 ± 0.14	349.~~20~~60 ± 0.25	1.029 ± 0.009

[a] Results from King *et al.*[26] and Karsili *et al.*[37]
[b] Obtained from the 0 K experimental results and calculated C_p values at the B3LYP/aug-cc-pVQZ level. The increased error from the 0 K results is due to uncertainty in the calculated heat capacities.

TABLE II. The experimentally measured frequencies of the Franck-Condon active normal modes for the doublet ground ($\tilde{X}$) and first excited ($\tilde{A}$) states of the three methylphenoxyl radicals. The calculated (B3LYP/aug-cc-pVQZ) harmonic frequencies are listed in parentheses below the measured frequency. All values are in cm^{-1}. Details describing the motion of these normal nodes are described in the text, while diagrams of those motions may be found in the Supplementary Material.

***o*-Methylphenoxyl Radical**	***m*-Methylphenoxyl Radical**	***p*-Methylphenoxyl Radical**
$\tilde{X}$ state	**$\tilde{X}$ state**	**$\tilde{X}$ state**
$\nu_{30} = 540 \pm 80$ *(577)*	$\nu_{31} = 560 \pm 50$ *(540)*	$\nu_{32} = 460 \pm 40$ *(461)*
$\nu_{31} = 540 \pm 80$ *(540)*	$\nu_{39} = 66 \pm 8$ *(81)*	
$\nu_{33} = 430 \pm 80$ *(453)*		
$\nu_{39} = 98 \pm 8$ *(106)*		
$\tilde{A}$ state	**$\tilde{A}$ state**	**$\tilde{A}$ state**
$\nu_{15} = 1220 \pm 130$ *(1312)*	$\nu_{15} = 1260 \pm 90$ *(1330)*	$\nu_{15} = 1240 \pm 90$ *(1320)*
$\nu_{32} = 480 \pm 190$ *(506)*	$\nu_{31} = 520 \pm 96$ *(542)*	$\nu_{32} = 460 \pm 80$ *(461)*
	$\nu_{32} = 520 \pm 96$ *(516)*	

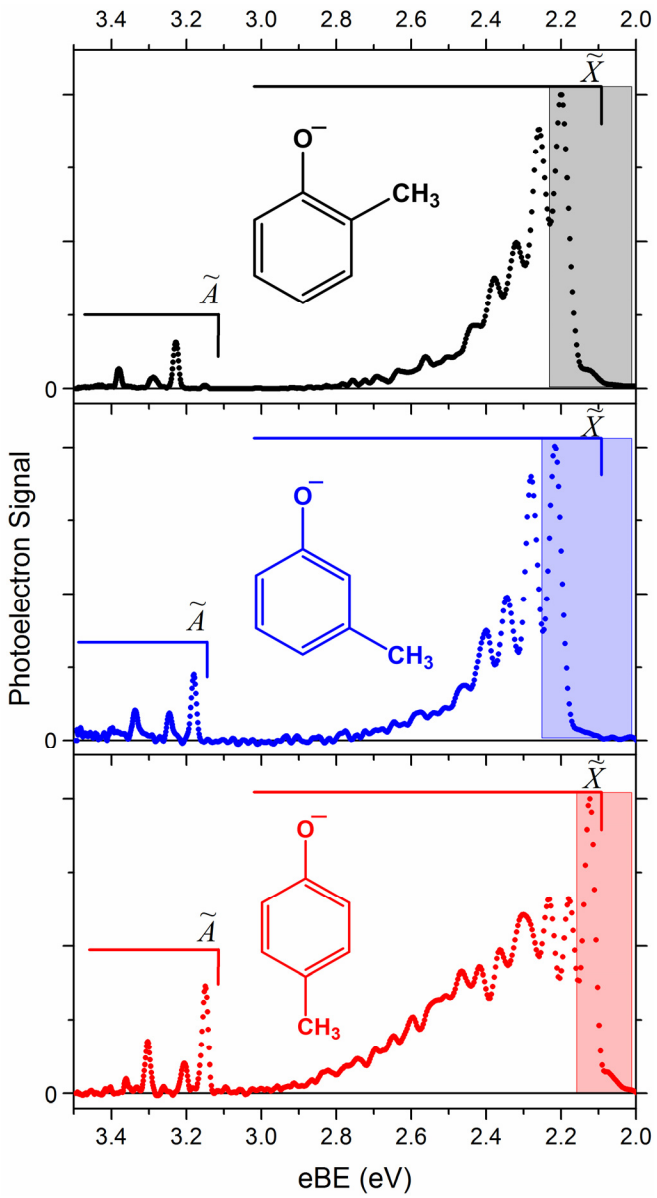

FIG. 1. The 355 nm photoelectron spectra of the three methylphenoxide anion isomers. These data were taken using the VMI photoelectron spectrometer. The $\tilde{X}$ refers to the ground doublet electronic state, while the $\tilde{A}$ refers to the first excited doublet electronic state of the corresponding neutral methylphenoxyl radicals. The data are reported as dots, with a line marking the baseline at zero. The shaded boxes indicate the energy range covered in Fig. 2.

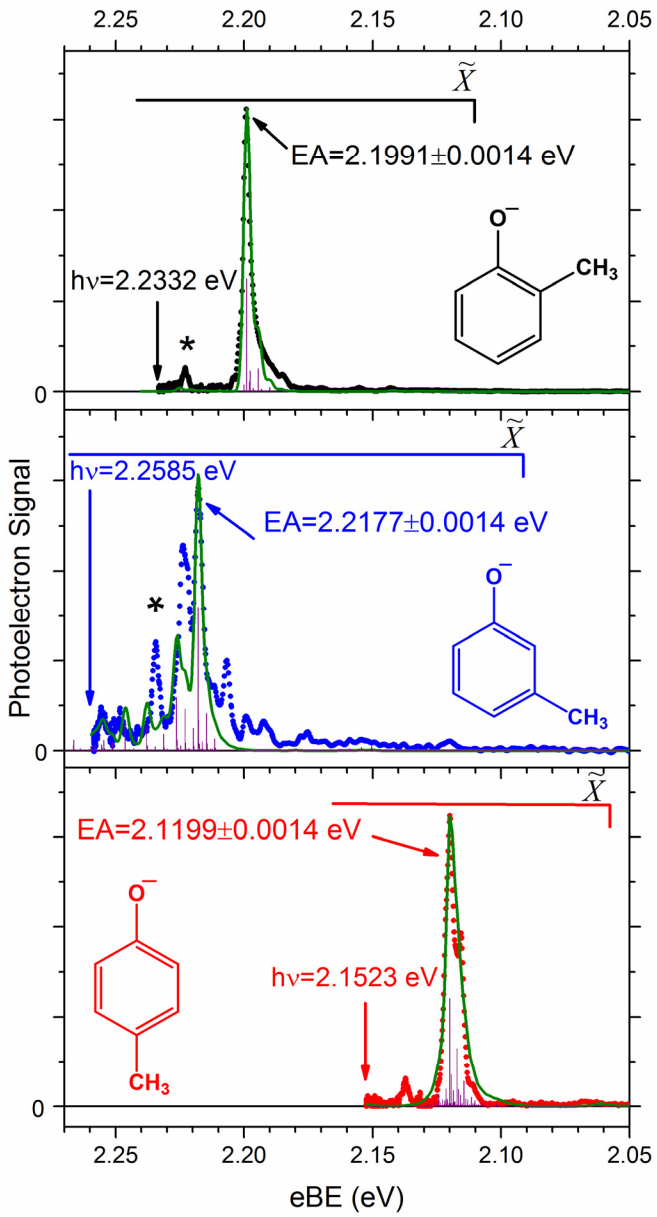

FIG. 2. The Slow Photoelectron Velocity-Map Imaging (SEVI) spectra of *o-, m-,* and *p-*methylphenoxide, allowing for the determination of the EAs of the corresponding methylphenoxyls. Experimental data are reported as dots, with a line marking the baseline at zero. Peaks labeled with an asterisk possibly represent the methyl hindered rotor vibrational transitions discussed in the text. Simulated Franck-Condon factors (T = 150 K) are shown as purple sticks and their convolution with the experimental resolution is shown in green. Note the x-axis only spans 2~~5~~20 meV, while Fig. 1 spanned 1.5 eV.

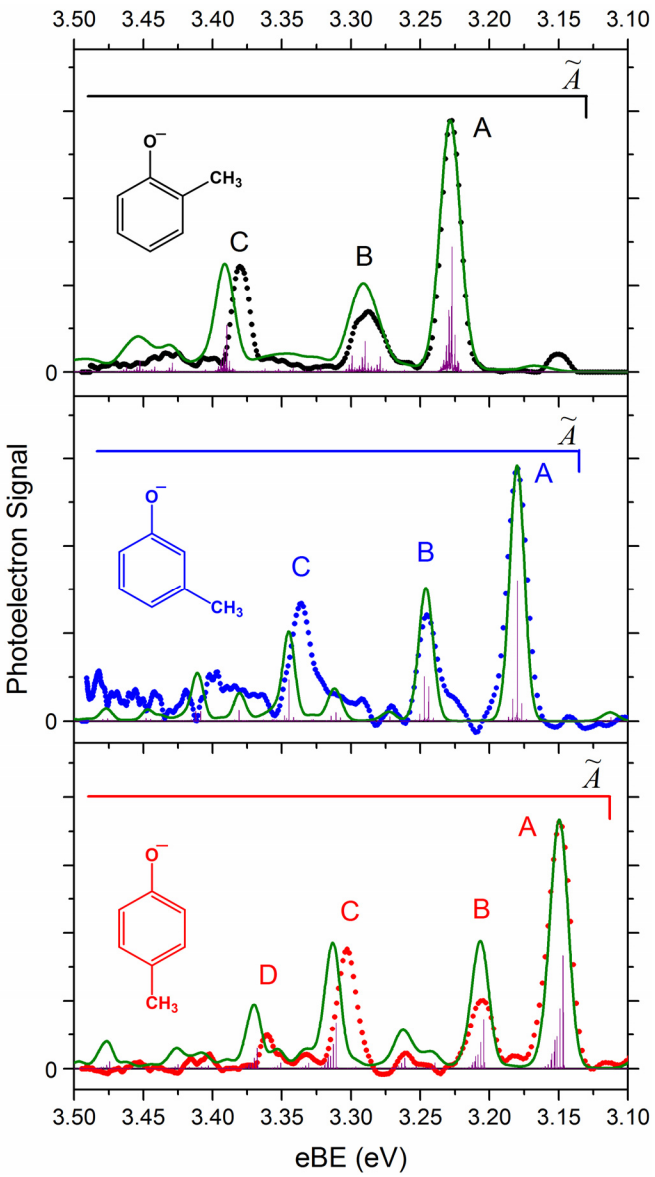

FIG. 3. The 355 nm anion photoelectron spectra of *o-, m-,* and *p*-methylphenoxide, examining the first excited doublet electronic states ($\tilde{A}$) of the methylphenoxyl radicals. Experimental data are shown as dots. Simulated Franck-Condon factors are shown as purple sticks and their convolution with the experimental resolution is shown in green.

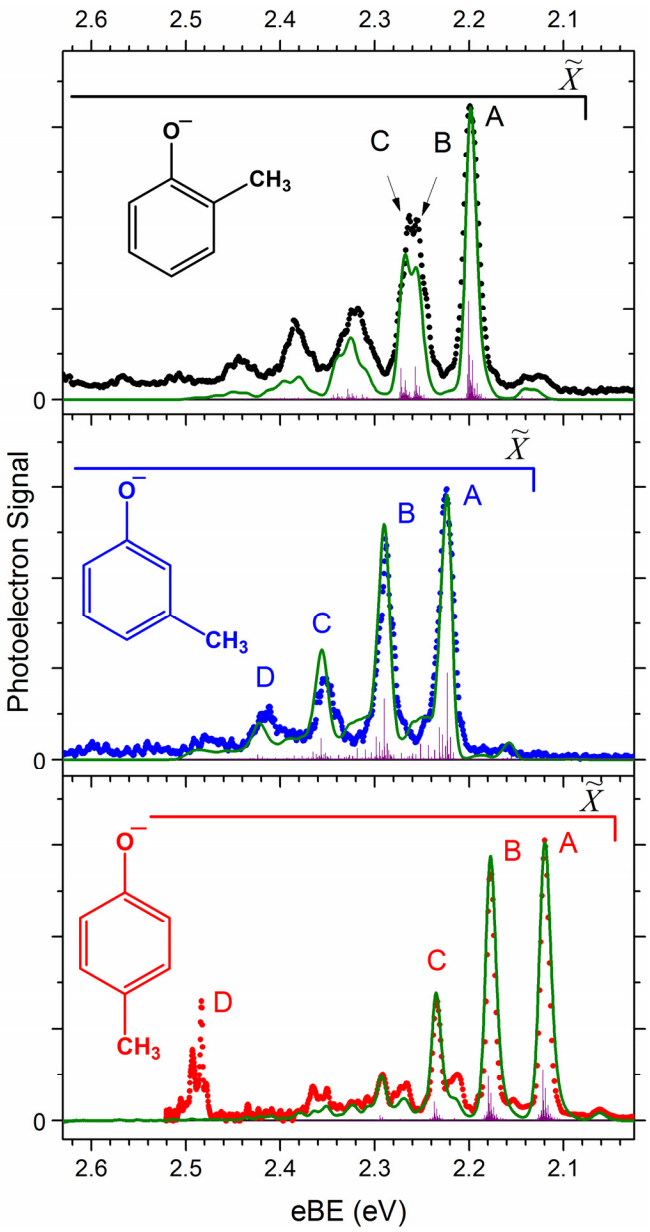

FIG. 4. The anion photoelectron spectra of *o-, m-,* and *p*-methylphenoxide, examining the ground doublet electronic states of the methylphenoxyls. Experimental data are displayed as dots. The top two panels were obtained with a photon energy of 3.408 eV using a hemispherical energy analyzer, while the bottom panel was collected using a VMI spectrometer with a photon energy of 2.520 eV. Simulated Franck-Condon factors are shown as purple sticks and their convolution with the experimental resolution is shown in green.

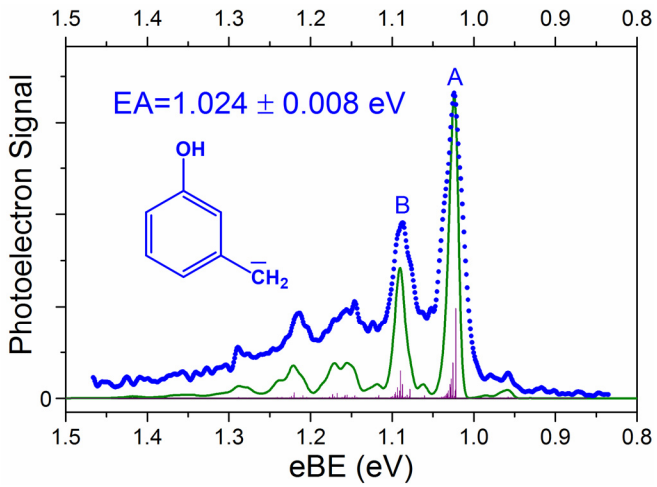

FIG. 5. Photoelectron spectrum of methyl deprotonated *meta*-methylphenol, taken with a photon energy of 3.408 eV and collected with a hemispherical energy analyzer. Experimental data are plotted with dots, the calculated Franck-Condon factors are shown as purple sticks, and the stick spectra convolved with the experimental resolution is shown in green.

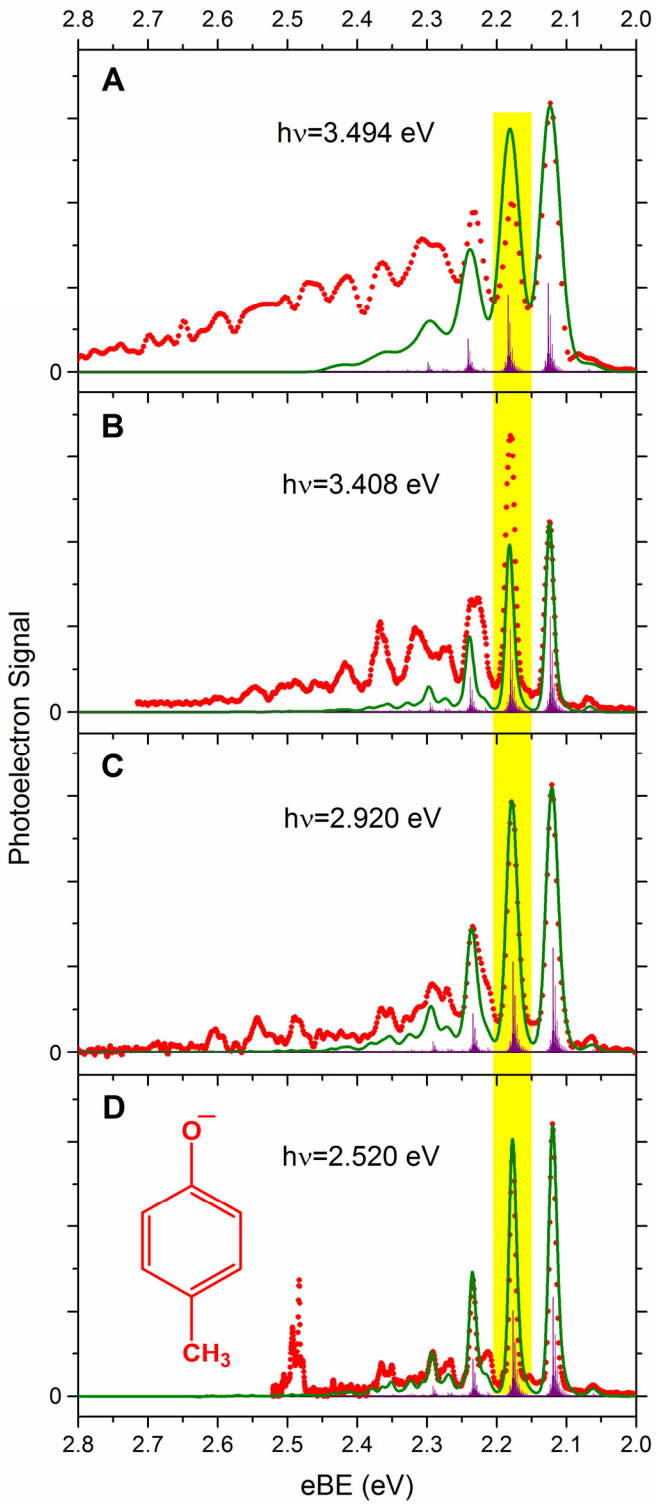

FIG. 6. Photoelectron spectra of *p*-methylphenoxide taken at a variety of photon energies, displaying a photon energy dependence as discussed further in the text. Data in panels **A**, **C**, and **D** (hν = 3.494 eV, 2.920 eV, and 2.520 eV) are obtained with a VMI spectrometer, while panel **B** (hν = 3.408 eV) was

collected with a hemispherical energy analyzer. Experimental data are shown as dots, while calculated Franck-Condon factors are shown as purple sticks and their convolution with experimental resolution shown in green. The highlighted peaks emphasize the intensity dependence on photon energy and are attributed to autodetachment, which is discussed further in the text.

REFERENCES

[1] M. Haeberlein and T. Brinck, J. Phys. Chem. **100**, 10116 (1996).
[2] C. Wang, D. Wang, Z. Wu, Z. Wang, C. Tang, and P. Zhou, Applied Catalysis A: General **476**, 61 (2014).
[3] E. O. Odebunmi and D. F. Ollis, Journal of Catalysis **80**, 56 (1983).
[4] V. M. L. Whiffen and K. J. Smith, Energy & Fuels **24**, 4728 (2010).
[5] C. Wang, Z. Wu, C. Tang, L. Li, and D. Wang, Catalysis Communications **32**, 76 (2013).
[6] V. M. L. Whiffen, K. J. Smith, and S. K. Straus, Applied Catalysis A: General **419–420**, 111 (2012).
[7] A. Hellweg, C. Hattig, I. Merke, and W. Stahl, J. Chem. Phys. **124**, 204305 (2006).
[8] G. Myszkiewicz, W. L. Meerts, C. Ratzer, and M. Schmitt, Phys. Chem. Chem. Phys. **7**, 2142 (2005).
[9] A. Hellweg and C. Hattig, J. Chem. Phys. **127**, 24307 (2007).
[10] H. Mizuno, K. Okuyama, T. Ebata, and M. Ito, J. Phys. Chem. **91**, 5589 (1987).
[11] T. Aota, T. Ebata, and M. Ito, J. Phys. Chem. **93**, 3519 (1989).
[12] K. Suzuki, Y. Emura, S.-i. Ishiuchi, and M. Fujii, J. Electron. Spectrosc. Relat. Phenom. **108**, 13 (2000).
[13] A. Oikawa, H. Abe, N. Mikami, and M. Ito, J. Phys. Chem. **88**, 5180 (1984).
[14] M. Pohl and K. Kleinermanns, Z. Phys. D: At., Mol. Clusters **8**, 385 (1988).
[15] C.-M. Tseng, Y. T. Lee, C.-K. Ni, and J.-L. Chang, J. Phys. Chem. A **111**, 6674 (2007).
[16] J. S. Wright, D. J. Carpenter, D. J. McKay, and K. U. Ingold, J. Amer. Chem. Soc. **119**, 4245 (1997).
[17] J. L. Lin, C. Li, and W. B. Tzeng, J. Chem. Phys. **120**, 10513 (2004).
[18] R. Tembreull and D. M. Lubman, Anal. Chem. **56**, 1962 (1984).
[19] H. S. Biswal, P. R. Shirhatti, and S. Wategaonkar, J. Phys. Chem. A **113**, 5633 (2009).
[20] J. Huang, K. Huang, S. Liu, Q. Luo, and W. Tzeng, J. Photochem. Photobiol. A **188**, 252 (2007).
[21] M. Ito and A. Oikawa, J. Mol. Struct. **126**, 133 (1985).
[22] H. M. Relles, D. S. Johnson, and J. S. Manello, J. Amer. Chem. Soc. **99**, 6677 (1977).
[23] T. Ebata and M. Ito, J. Phys. Chem. **96**, 3224 (1992).
[24] M. Gerhards, B. Kimpfel, M. Pohl, M. Schmitt, and K. Kleinermanns, J. Mol. Struct. **270**, 301 (1992).
[25] R. J. Lipert and S. D. Colson, J. Phys. Chem. **93**, 3894 (1989).
[26] G. A. King, A. L. Devine, M. G. D. Nix, D. E. Kelly, and M. N. R. Ashfold, Phys. Chem. Chem. Phys. **10**, 6417 (2008).
[27] L. A. Angel and K. M. Ervin, J. Phys. Chem. A **110**, 10392 (2006).
[28] A. Chandra and T. Uchimaru, Int. J. Mol. Sci. **3**, 407 (2002).
[29] R. M. B. d. Santos and J. A. M. Simoes, J. Phys. Chem. Ref. Data **27**, 707 (1998).
[30] L. S. Richard, C. E. S. Bernardes, H. P. Diogo, J. P. Leal, and M. E. Minas da Piedade, J. Phys. Chem. A **111**, 8741 (2007).
[31] K. B. Wiberg, G. B. Ellison, J. M. McBride, and G. A. Petersson, J. Phys. Chem. A **117**, 213 (2012).
[32] S. A. Kudchadker, A. P. Kudchadker, R. C. Wilhoit, and B. J. Zwolinski, J. Phys. Chem. Ref. Data **7**, 417 (1978).
[33] J. D. Cox, Pure Appl. Chem. **2**, 125 (1961).
[34] K. M. Ervin and V. F. DeTuri, J. Phys. Chem. A **106**, 9947 (2002).

[35] M. Fujio, R. T. McIver, and R. W. Taft, J. Amer. Chem. Soc. **103**, 4017 (1981).
[36] T. B. McMahon and P. Kebarle, J. Amer. Chem. Soc. **99**, 2222 (1977).
[37] T. N. V. Karsili, A. M. Wenge, B. Marchetti, and M. N. R. Ashfold, Phys. Chem. Chem. Phys. **16**, 588 (2014).
[38] J. B. Kim, T. I. Yacovitch, C. Hock, and D. M. Neumark, Phys. Chem. Chem. Phys. **13**, 17378 (2011).
[39] R. F. Gunion, M. K. Gilles, M. L. Polak, and W. C. Lineberger, Int. J. Mass Spectrom. Ion Processes **117**, 601 (1992).
[40] D. G. Leopold, K. K. Murray, A. E. S. Miller, and W. C. Lineberger, J. Chem. Phys. **83**, 4849 (1985).
[41] K. M. Ervin and W. C. Lineberger, in *Advances in Gas Phase Ion Chemistry*, edited by N. G. Adams, and L. M. Babcock (JAI Press, Greenwich, 1992), pp. 121.
[42] B. Ruscic, A. F. Wagner, L. B. Harding, R. L. Asher, D. Feller, D. A. Dixon, K. A. Peterson, Y. Song, X. Qian, C.-Y. Ng, J. Liu, W. Chen, and D. W. Schwenke, J. Phys. Chem. A **106**, 2727 (2002).
[43] C. T. Wickham□Jones, K. M. Ervin, G. B. Ellison, and W. C. Lineberger, J. Chem. Phys. **91**, 2762 (1989).
[44] D. M. Neumark, K. R. Lykke, T. Andersen, and W. C. Lineberger, Physical Review A **32**, 1890 (1985).
[45] K. M. Ervin, I. Anusiewicz, P. Skurski, J. Simons, and W. C. Lineberger, J. Phys. Chem. A **107**, 8521 (2003).
[46] J. Cooper and R. N. Zare, J. Chem. Phys. **48**, 942 (1968).
[47] L. Sheps, E. M. Miller, and W. C. Lineberger, J. Chem. Phys. **131**, 064304 (2009).
[48] Y.-J. Lu, J. H. Lehman, and W. C. Lineberger, J. Chem. Phys. **142**, 044201 (2015).
[49] A. T. J. B. Eppink and D. H. Parker, Rev. Sci. Instrum. **68**, 3477 (1997).
[50] H. Hotop and W. C. Lineberger, J. Phys. Chem. Ref. Data **14**, 731 (1985).
[51] C. Blondel, W. Chaibi, C. Delsart, C. Drag, F. Goldfarb, and S. Kröger, Eur. Phys. J. D **33**, 335 (2005).
[52] D. M. Neumark, J. Phys. Chem. A **112**, 13287 (2008).
[53] M. J. Frisch, G. W. Trucks, H. B. Schlegel, G. E. Scuseria, M. A. Robb, J. R. Cheeseman, G. Scalmani, V. Barone, B. Mennucci, G. A. Petersson, H. Nakatsuji, M. Caricato, X. Li, H. P. Hratchian, A. F. Izmaylov, J. Bloino, G. Zheng, J. L. Sonnenberg, M. Hada, M. Ehara, K. Toyota, R. Fukuda, J. Hasegawa, M. Ishida, T. Nakajima, Y. Honda, O. Kitao, H. Nakai, T. Vreven, J. A. Montgomery Jr., J. E. Peralta, F. Ogliaro, M. J. Bearpark, J. Heyd, E. N. Brothers, K. N. Kudin, V. N. Staroverov, R. Kobayashi, J. Normand, K. Raghavachari, A. P. Rendell, J. C. Burant, S. S. Iyengar, J. Tomasi, M. Cossi, N. Rega, N. J. Millam, M. Klene, J. E. Knox, J. B. Cross, V. Bakken, C. Adamo, J. Jaramillo, R. Gomperts, R. E. Stratmann, O. Yazyev, A. J. Austin, R. Cammi, C. Pomelli, J. W. Ochterski, R. L. Martin, K. Morokuma, V. G. Zakrzewski, G. A. Voth, P. Salvador, J. J. Dannenberg, S. Dapprich, A. D. Daniels, Ö. Farkas, J. B. Foresman, J. V. Ortiz, J. Cioslowski, and D. J. Fox, Gaussian 09 Rev. B01, 2009, see www.gaussian.com
[54] A. D. Becke, J. Chem. Phys. **98**, 5648 (1993).
[55] K. M. Ervin, PESCAL, Fortran Program for Franck-Condon Analysis of Molecular Photoelectron Spectra, 2010, see http://wolfweb.unr.edu/~ervin/pes/
[56] T. E. Sharp and H. M. Rosenstock, J. Chem. Phys. **41**, 3453 (1964).
[57] E. B. Wilson, Jr., Phys. Rev. **45**, 706 (1934).
[58] P. Chen, *Unimolecular and Bimolecular Reactions Dynamics* (John Wiley & Sons, Chichester, 1994), 371.
[59] M. J. Travers, D. C. Cowles, E. P. Clifford, G. B. Ellison, and P. C. Engelking, J. Chem. Phys. **111**, 5349 (1999).
[60] A. Sanov, Annu. Rev. Phys. Chem. **65**, 341 (2014).
[61] J. B. Kim, P. G. Wenthold, and W. C. Lineberger, J. Phys. Chem. A **103**, 10833 (1999).
[62] H.-T. Liu, C.-G. Ning, D.-L. Huang, P. D. Dau, and L.-S. Wang, Angew. Chem. Int. Ed. **52**, 8976 (2013).
[63] D.-L. Huang, H.-T. Liu, C.-G. Ning, and L.-S. Wang, J. Chem. Phys. **142**, 124309 (2015).
[64] M. L. Weichman, J. B. Kim, and D. M. Neumark, J. Phys. Chem. A **119**, 6140 (2015).
[65] M. G. D. Nix, A. L. Devine, B. Cronin, R. N. Dixon, and M. N. R. Ashfold, J. Chem. Phys. **125**, 133318 (2006).
[66] W. M. Haynes, *CRC Handbook of Chemistry and Physics* (CRC Press, New York, 2016-2017).